ACTA
AMAZONICA

http://dx.doi.org/10.1590/1809-4392202400641

BIODIVERSITY AND CONSERVATION | ORIGINAL ARTICLE

Scale by scale, river by river: On the taxonomy, osteology and distribution of the Amazonian snake *Helicops acangussu*

Nathalie CITELI[1,2,3]*, Julia KLACZKO[3], Angele R. MARTINS[3,4], José Rancés CAICEDO PORTILLA[5], Alessandra SILVEIRA[6], Ricardo Tadeu LOPES[6], Reuber A. BRANDÃO[2]

[1] Universidade Católica de Brasília, Laboratório de Coleção Zoológica, Taguatinga, 71966-700 DF, Brazil
[2] Universidade de Brasília, Laboratório de Fauna e Unidades de Conservação, Brasília, 70910-900 DF, Brazil
[3] Universidade de Brasília, Laboratório de Anatomia Comparada dos Vertebrados, Brasília, 70910-900 DF, Brazil
[4] Universidade Federal do Rio de Janeiro, Departamento de Vertebrados, Museu Nacional, Quinta da Boa Vista 20940-040 RJ, Brazil
[5] Instituto Amazónico de Investigaciones Científicas SINCHI, Colección de Reptiles, Leticia, Amazonas, 110311, Colombia
[6] Universidade Federal do Rio de Janeiro, Laboratório de Instrumentação Nuclear (LIN), Ilha do Fundão, 21910240 RJ, Brazil
* Corresponding author: citelissaura@gmail.com

ABSTRACT

Helicops acangussu was described in 2022 based on 27 specimens collected on the left bank of the Madeira River, state of Rondônia, Brazil. During visits to South American collections, we found 34 new specimens, most from regions about 1000 km away from the type locality, in the Amazon region of Colombia (municipality of Leticia) and Brazil (municipalities of Tabatinga and Presidente Figueiredo). The detailed examination of the material from these new populations allowed us to provide the first description of the skull, lower jaw and cervical osteology for the species, as well as to expand the external morphological variation of meristic and biometric characters and provide new data on the morphology of the hemipenis. We show that *Helicops acangussu* is a species with a solid taxonomy, but with pronounced intraspecific variation in hemipenis morphology and a wide distribution in the Amazon region.

KEYWORDS: cervical vertebrae, Dipsadidae, hemipenis variation, lower jaw, Serpentes, watersnake

Escama por escama, rio por rio: sobre a taxonomia, osteologia e distribuição da serpente amazônica *Helicops acangussu*

RESUMO

Helicops acangussu foi descrita em 2022 com base em 27 exemplares coletados na margem esquerda do Rio Madeira, estado de Rondônia, Brasil. Durante visitas a coleções sul-americanas, encontramos 34 novos exemplares, em sua maioria provenientes de regiões distantes cerca de 1000 km da localidade tipo, na região amazônica da Colômbia (município de Leticia) e do Brasil (municípios de Tabatinga e Presidente Figueiredo). O exame detalhado do material dessas novas populações nos permitiu fornecer a primeira descrição do crânio, mandíbula e osteologia cervical para a espécie, bem como a ampliação da variação morfológica externa de caracteres merísticos e biométricos, além de novos dados sobre a morfologia do hemipênis. Mostramos que *Helicops acangussu* é uma espécie com taxonomia sólida, mas com acentuada variação intraespecífica na morfologia dos hemipênis e ampla distribuição na região Amazônica.

PALAVRAS-CHAVE: vértebras cervicais, Dipsadidae, variação do hemipênis, maxilar inferior, Serpentes, cobra d'água

INTRODUCTION

Helicops Wagler, 1828 is a neotropical genus of aquatic snakes with 21 species distributed exclusively in South America (Nogueira *et al*. 2019; Moraes-da-Silva *et al*. 2019; 2021; 2022). Over the last decade, the knowledge about this genus has been significantly expanded concerning morphology (Garcia-Cobos 2021; Citeli *et al*. 2022), reproduction (Braz *et al*. 2016; Garcia-Cobos 2020), and taxonomy (Kawashita-Ribeiro *et al*. 2013; Costa *et al*. 2016; Moraes-da-Silva *et al*. 2019; 2021; 2022). *Helicops acangussu* Moraes-da-Silva, Walterman, Citeli, Nunes & Curcio 2022 was the latest species described for the genus, based on 27 specimens from the left bank of the upper Madeira River in Rondônia state, Brazil, collected during a wildlife rescue operation associated

CITE AS: Citeli, N.; Klackzo, J.; Martins, A.R.; Caicedo Portilla, J.R.; Silveira, A.; Lopes, R.T.; Brandão, R.A. 2025. Scale by scale, river by river: On the taxonomy, osteology and distribution of the Amazonian snake *Helicops acangussu*. *Acta Amazonica* 55: e55bc24064.

with the Santo Antônio Dam, Rondônia state, Brazil. The specimens of the type series had been previously identified as *Helicops hagmanni* Roux 1910 in the Brazilian herpetological collections at Museu Paraense "Emilio Goeldi" (MPEG) and Universidade Federal de Rondônia (UFRO-H) (Moraes-da-Silva *et al.* 2022).

Helicops acangussu was tentatively allocated to the group composed of *Helicops* bearing dorsal spotted patterns (Moraes-da-Silva *et al.* 2022), including *H. hagmanni*, *Helicops leopardinus* (Schlegel, 1837), *Helicops pastazae* (Schlegel, 1834), *Helicops petersi* Rossman, 1976, *Helicops polylepis* Günther, 1861, *Helicops yacu* Rossman and Dixon, 1975 (all Amazonian species), and *Helicops danieli* Amaral, 1937 (restricted to the Colombian transandine region) (Rossman 2002; Citeli *et al.* 2022). However, *H. acangussu* can be distinguished from these species mainly by meristic and colour pattern variation (Citeli 2022; Moraes-da-Silva *et al.* 2022).

Although the description of *H. acangussu* is consistent, the genus is known to present morphological variation, as polymorphisms and overlapping diagnostic characters among species have been described (e.g., Rossman and Dixon 1975; Rossman 1976; Kawashita-Ribeiro *et al.* 2013; Moraes-da-Silva *et al.* 2022). Therefore it is important to record the intraspecific morphological variation of *Helicops* taxa throughout their distribution range, including geographic clines, to determine their patterns of variation in morphology and propose correct criteria for species delimitation (e.g., Allsteadt *et al.* 2006; Ennen *et al.* 2014)

During visits to South American herpetological collections to study Amazonian species of *Helicops*, we found 34 new specimens of *H. acangussu*, a topotype and 33 from locations far from its type locality and originally proposed distribution range. After a careful analysis of these new specimens, we present in here (i) data on the geographical variation in the external morphology of *H. acangussu*; (ii) the first osteological description of the skull, lower jaw and cervical vertebrae for this species; (iii) new data on the hemipenis morphology, complementing the description by Moraes-da-Silva *et al.* (2022); and (iv) an update on the geographical distribuition of the species in the Amazon region.

MATERIAL AND METHODS

Sampling and meristic variation

We analyzed a sample of 34 specimens of *Helicops acangussu* (24 females and 10 males), of wich 32 were collected in the municipalities of Leticia (Amazonas departament, Colombia) and Tabatinga (Amazonas state, Brazil) and deposited in the reptiles collection at Instituto Amazónico de Investigaciones Científicas SINCHI (SINCHI-R), in Leticia (Colombia), where they had been previously identified as *H. leopardinus*. Another specimen (a male identified as *Helicops hagmanni* collected in Presidente Figueiredo, Amazonas state, Brazil) was housed in the herpetological collection at Instituto Nacional de Pesquisas da Amazônia (INPA-H), in Manaus (Amazonas, Brazil). To obtain skull data, we also examined a female topotype housed at the Museu Paraense "Emílio Goeldi" (MPEG) in Belém, Pará, Brazil. This specimen was collected at the same time as the individuals in the type series. Institutional abbreviations follow Sabaj (2020). We followed Dowling (1951) and Moraes-da-Silva *et al.* (2019; 2021) for scale counts, Citeli (2022) and Moraes-da-Silva *et al.* (2019; 2021) for body and head trait measurements, and Moraes-da-Silva *et al.* (2022) for dorsal spots on dorsum counts. All measurements were taken with a digital caliper to the nearest 0.01 mm, except for snout–vent length (SVL) and tail length (TL) measurements, where we used a flexible ruler. The sex of individuals with no everted hemipenis was identified through an incision at the base of the tail to detect the presence of hemipenes and retractor muscles.

Skull and hemipenial morphology

The new data on the hemipenial morphology of *H. acangussu* were taken from three preserved specimens (SINCHI-R 01025, SINCHI-R 01026, from Letícia, and INPA 31415, from Presidente Figueiredo). We extracted, everted, and prepared the hemipenis following Pesantes (1994) and Zaher and Prudente (2003). We filled the fully everted hemipenis with petroleum jelly to visualize the ornamentation structures. The organs were then photographed and measured using the ImageJ software version 1.8.0 (Rasband 2016). We followed the terminology by Zaher (1999) for hemipenis structure description and Citeli *et al.* (2022) for the measurements.

The heads of two individuals (INPA 31415 and the topotype MPEG 25586, from Rondônia) were X-rayed in 3D with high-resolution microCT (micro-computed tomography) scanning procedures using a Bruker SkyScan 1273 at Instituto Alberto Luiz Coimbra de Pós-graduação e Pesquisa de Engenharia (COPPE) at Universidade Federal do Rio de Janeiro, in Rio de Janeiro (Brazil). The scans were made with an X-ray beam with 50kV source voltage and 220 µA current without the use of a filter. Rotation steps of 0.3 degrees were used with a frame averaging of 5, recorded over a 180° rotation, resulting in 688 projections of 191 ms exposure time each and a total scan duration of 0:34:11s. The microCT-dataset was reconstructed using N-Recon software (Bruker MicroCT) resulting in 1723-1741 slices and rendered in three dimensions through the aid of CTVox for Windows 64 bits version 2.6 (Bruker MicroCT). We used Fiji Software and 3D Slicer and followed Buser *et al.* (2020) for segmentation.

The terminology for description of skull osteology follows Cundall and Irish (2008), and for cervical vertebrae follows Holman (2000).

Distribution map

We acquired the reference geographic coordinates of the municipalities in which the new specimens were collected from Google Earth. We used the software Quantum GIS 3.16 (QGIS) to produce the map using SIRGAS 2000. To identify which hydrographic basins were included in the species' distribution, we used the shape of the South American basins available at HydroBASINS (Lehner and Grill 2013).

RESULTS

Meristic variation

Among the 32 examined specimens from Leticia and Tabatinga, the largest specimen was a female with SVL = 620 mm and the smallest a juvenile female with SVL = 110 mm. The meristic characteristics (Figure 1) were as follows: scale rows usually in a 19/19/17 series (n = 28), and more rarely in 21/19/17 (n = 2), 20/20/17 (n = 1) or 19/19/16 (n = 1); single preocular (n = 31), rarely two (n = 1); two postoculars (n = 30) and three in an asymmetric specimen (n = 1); temporal formula usually 2+3 (n = 24), rarely 2+2 (n = 1) or 1+3 (n = 1), 3/2+3 (n = 4), 2+2/3 (n = 1) or 1/2+3 (n = 1); supralabials eight (n = 32); fourth supralabial usually contacting orbit (n = 32); pairs of chinshields (n = 32); infralabials usually 10 (n = 28), rarely 11 (n = 2), in asymetric specimens 10/11 (n =1) or 12/11 (n = 1); first to fifth infralabials contacting anterior pair of chinshields (n = 26), in asymetric specimens first to fourth (n = 4) and first to sixth (n = 2); fifth and sixth infralabials contacting posterior pair of chinshields (n =27), rarely only fifth (n= 3) or sixth (n = 1), in asymetric specimen (n = 1); posterior separated by one pair of intergenial scales (n = 32); ventral scales 126–133 in females (n = 22), 122–130 in males (n = 9); subcaudals 42–65 in females (n = 22), 56–72 in males (n = 9); cloacal plate always divided (n = 32); subcaudals divided (throughout the tail) (n = 32); nasal semidivided and separated by internasal scales. The eye diameter was the same size as its distance to the oral border (eye-mouth distance) (n = 32); internasal wider than long, triangular in shape, in contact with the rostral (n = 32); loreal as long as wide (n = 32); dorsum and tail covered by five rows of circular darker spots (n = 32); dorsal spots 2–3 scales long (n = 30), rarely six when two rows of spots are connected (n = 2); dorsal spot number 47–57 in females (n = 22), 48–60 in males (n = 9); whitish belly with alternating and irregular bars (n = 32); ventral bars touch the second scale row (n = 32); head dorsum brownish with black pigments forming an arrow-like design, tip of head with a light snout spot slightly triangular in shape (n = 32); supralabials brownish with darker pigments more restricted to the sutures (n = 28) or homogeneous brownish (n = 4); infralabials whitish with brownish pigments more restricted to the sutures (n = 32); snout showing a triangular-shaped light spot (n = 32).

The features of the male from Presidente Figueiredo (Figure 1b,c) were generally in accordance with most of the reported data for *H. acangussu*, including the sample from Leticia/Tabatinga, except in that it was the only specimen with a scale row series of 21/21/17. It also had the lowest recorded number of ventral scales (117), darker and larger spots 3.5–4.0 scales long and in smallest number (29) along the body.

Figure 1. *Helicops acangussu* (SINCHI-R 3169) from Leticia, Amazonas, Colombia: **A** – live image. Male specimen of *Helicops acangussu* (INPA 31425) from Presidente Figueiredo, Amazonas, Brazil: **B** – dorsal view; **C** – ventral view. Scale bar = 2 cm (B, C). Credit: Dario Alarcón (A).

Remarks on scalation

In the type series, ventral scalation count was 124–129 in females and 121–128 in males, subcaudal scale count was 40–43 in females and 52–67 in males, number of dorsal spots on the trunk was 36–42 in females and 35–47 in males (see Moraes-da-Silva *et al.* 2022). Here we expanded the variation of these traits, increasing the maximum ventral scale count to 133 in females and expanding the range of ventral scale number to 117–130 in males, while the maximum number of subcaudal scales was increased to 65 in females and to 72 in males; and the range of the number of dorsal spots on the trunk was expanded to 36–57 in females and to 29–60 in males.

Skull morphology

The skull of the two specimens from Rondônia and Presidente Figueiredo was widest at the mid-anterior portion at the level of the orbits in dorsal view. **Premaxilla** (Figure 2): edentulous, approximately triangular in anterior view with concave lateral edges, almost in contact with nasals dorsally and septomaxillae ventrally (at the vomerine processes), pierced by three ventral foramina, two of them opening dorsolaterally or not; medial lamina of nasal process moderate, projected upwards and posteriorly and exceeding the anterior limit of the septomaxillae in lateral view; vomerine process double at posterior end, with conspicuous separation from each other; transverse (=maxillary) processes wide, flattened almost in contact with maxillae. **Septomaxilla** (Figure 2c): anterior lamina fits laterally to each arm of the vomerian process of the premaxilla; almost in contact with premaxilla ventrally; conchal process rectangular in lateral view, projected dorsolaterally, inflecting medially, not contacting nasals or prefrontals; articulates with frontals posteriorly, participating in the prokinetic joint; dorsally in contact with the nasal septum of nasals. **Vomers** (Figure 2c): premaxillary process of each vomer not in contact medially, tapered anteriorly and reaching or not the dorsal lamina of the vomerine processes of the premaxilla, convex laterally, delimiting the medial edge of the olfactory capsule; caudal processes of vomer reduced and project posteriorly in medial line, constituting exochoanal fenestra; dorsoposterior lamina pierced by several foramina of different sizes. **Nasals** (Figure 2a-b): dorsal lamina elongate with concave anterior edges and oblique posterior edges; mid-anterior portion almost contacts the nasal process of the premaxilla ventrally and does not contact the frontals posteriorly; does not form the prokinetic joint; nasal septum double, ventrally supported by the middorsal surface of the septomaxillae. **Prefrontals** (Figure 2a-b): dorsoventrally expanded, contacting the frontal at its dorsoposterior portion, and the maxillae and palatines ventrally; descending lamina anteroposteriorlly compressed, with medial process towards the prokinetic joint (but not touching it) and pierced by a wide lacrimal foramen. **Frontals** (Figure 2a-b): rectangular in dorsal view, pierced or not pierced by small foramina at the dorsal lamina; contacts prefrontals anterolaterally and the parietal posteriorly; not in contact with postorbital; ventrally in contact with septomaxila at the prokinetic joint, which is composed exclusively by these two bones, since frontals do not contact nasals; anteriorly, supra and subolfactory laminae converge medially, forming the interolfactory pillar, restricted to the whole internal extension of the frontal. **Postorbitals** (Figure 2b): well developed, delimiting the orbital cavity posteriorly; composed by a wide vertical portion; dorsal process absent; ventrally descends to almost contact the maxillae. **Parietal** (Figure 2a-b): wide, dorsoanterior edge concave and attached to frontals; anterolateral edge in contact with postorbital; in contact with supraoccipitals posteriorly, posterolaterally to prootics, and ventromedially to parabasisphenoid; dorsal surface smooth with two parietal crests that converge posteriorly; dorsal lamina tapers posteromedially, being irregularly convex at the posterior end; dorsally pierced by two or three small foramina. **Supraoccipital** (Figure 2a): fused into a single unit and pentagonal, contacting the parietal anteriorly, prootics laterally and exoccipitals posteriorly; dorsoanterior edge irregularly convex; lateral margins contacting the medial limit of the supratemporal; dorsally with a longitudinal and an oblique crest, which makes its posterior portion ventrally positioned; dorsally pierced by four or six small foramina. Forms the dorsal limit of the otic capsule, specifcally the medial semicicruclar canal and the *cavum vestibuli*. **Exoccipitals** (Figure 2a): irregular in dorsal view, comprising the dorsal edge of the foramen magnum; each exoccipital contacting the supraoccipital anteriorly, the basioccipital ventrally and the prootic laterally; two to four craniocervical foramina ventrolaterally located at each exoccipital. Its dorsal surface participates in the formation of the roof of the posterior semicircular canal. **Basioccipital** (Figure 2c): hexagonal in ventral view, contributing to the posterior portion of the braincase floor, as well as the medial portion of the occipital condyle; contacts the parabasisphenoid complex anteriorly, prootics and exoccipitals laterally, and atlas posteriorly, where it composes the ventral edge of the foramen magnum; ventral crests conspicuous and present at each side; ventral surface pierced by two small foramina. **Parabasisphenoid** (Figure 2c): lanceolate with blunt anterior edge, contacting frontals dorsoanteriorly, parietal and prootic laterally, and basioccipital posteriorly; ventral longitudinal crest present; ventrally pierced by a pair of wide posterior Vidian foramina, and a small pair of foramina slightly anterior to the Vidian canal foramen might represent the anterior Vidian canal foramen. **Prootics** (Figure 2b): irregular, contacting the parietal anteriorly, parabasisphenoid and basioccipital ventrally, supraoccipital and exoccipital posterolaterally; anterior portion of supratemporal lies on its whole dorsal surface; posteroventral limit forms the anterior edge of the foramen ovale; laterosphenoid present and separating the wide foramen for the maxillary branch from the mandibular branch of the trigeminal nerve foramina; two small foramina anterior to the mandibular branch; internally at *cavum vestibulii* a wide statolythic mass present at each side. **Columela auris**: small and slender bone inserted in fenestra ovalis, composed of the posterolateral portion of the prootics and anterolateral portion of the exoocipitals; it crosses the fenestra ovalis towards the quadrate, but not in contact with it. **Maxilla** (Figure 2): ventrolateral to the skull; in lateral view, extends slightly posterior to the anterior tip of the premaxilla until 2/3 of the extension of the parietal; posterior tip attached to the ventroanterior tip of the ectopterygoid trough the wide and dorsoventrally flattened ectopterygoid process; palatine process at medial portion with dorsal contact with prefrontal; lateral surface concave and pierced by a single foramen; 17-18 posteriorly curved teeth.

Palatine (Figure 2c): about half the length of the maxilla, in anterodorsal contact with prefrontal; posterior tip slightly forked and attached to anterodorsal tip of the pterygoid; maxillary process of palatine present; 8-9 teeth; choanal process absent. **Pterygoids** (Figure 2): each pterygoid located posterior to palatine, with its posterior portion enlarged and exceeding the posterior limits of the skull; 19 teeth, smaller than those in the maxillary and palatine; ectopterygoid fits to last 2/3 of the dorsal surface of the pterygoid. **Ectopterygoids** (Figure 2): anterior portion bifurcated and attached to ectopterygoid process of maxilla, reaching the level of the penultimate teeth; ventrally, attached to the dorsomedial portion of the pterygoid. **Supratemporals** (Figure 2a-b): elongated, ventrally attached to midposterior portion of the prootics and posteriorly reaching the posterior portion of the axis; articulates lateroposteriorly with the quadrate. **Quadrates** (Figure 2): Elongated and vertically positioned; proximal portion enlarged, medially articulated with posterodorsal portion of the supratemporal; distally slightly enlarged, articulating with the glenoid cavity of the retroarticular process (Figure 3) of the mandible; lateral lamina twisted along its axis, oriented to the posterior portion of the skull ventrally and with a short articulatory process posteriorly; lateral lamina not pierced by any foramen. **Compound bone** (Figure 3): connected to skull through the glenoid cavity posteriorly; anterior portion projected as a tapered process, which fits into the dentary, extending until the level of the ninth tooth; lateral lamina concave; midventral lamina contacting angular; mandibular fossa relatively deep, with one anterior internal foramen; surangular crest higher than prearticular crest; retroarticular process short, medially curved, blunt posteriorly, and posteriorly pierced by a small foramen. **Dentaries** (Figure 3): with 22–23 teeth that gradually slightly decrease in size posteriorly; posterolaterally in contact with compound bone, where it is forked, one process extending dorsally and the other (three times longer than the first) ventrally; anterior end fits between the two latter processes; mentonian foramen located laterally below the sixth or seventh tooth; posteromedial end does not contact the angular; splenial fits medially to its posterior region; Meckel's groove opening at level of fourth or fifth tooth. **Splenials** (Figure 3b): anterior portion fits into dentary through a tapering process, until seventh tooth, with its posterior end attached to the angular; posterior region pierced by the milohyoid foramen. **Angulars** (Figure 3b): triangular, anterior portion extending until the level of the fourteenth tooth; anteroventral portion pierced by the milohyoid foramen. **Atlas**: pair of dorsally unfused neural arches; transverse process conspicuous present at centrum (Figure 4h); tapered dorsolateral process present at each neural arch (Figure 4a-d); intercentrum I (Figure 4a-c) wide, with ventral tapered projection; pierced by three foramina. **Axis**: centrum perforated by a single foramen; spinal process well-developed reaching half the extension of posterior cervical vertebrae (Figure 4f-h); odontoid process blunt anteriorly (Figure 4f,h-i); intercentra II rounded or blunt and unfused to centrum, intercentra III fused to intercentrum II and pointed (Figure 4g-h).

Hemipenial morphology

Most of the features observed in the hemipenes of specimens SINCHI-R 01025 (right) and SINCHI-R 01026 (right) were in accordance with the original species description, however, none of the two organs showed significantly asymmetrical lobes, nor rows of papillae at the apex of the lobes, as presented in the original description (see Moraes-da-Silva *et al.* 2022). For specimens SINCHI-R 01025 and 01026, respectively, the total length of the hemipenes was 28.10 and 24.5 mm, the width measured at the hemipenial body and before capitation was 10.4 and 5.0 mm, the mean length of the lobes was 10.8 and 7.5 mm, corresponding to 38% and 30% of the total length of the organ. The sulcus spermaticus bifurcates at the

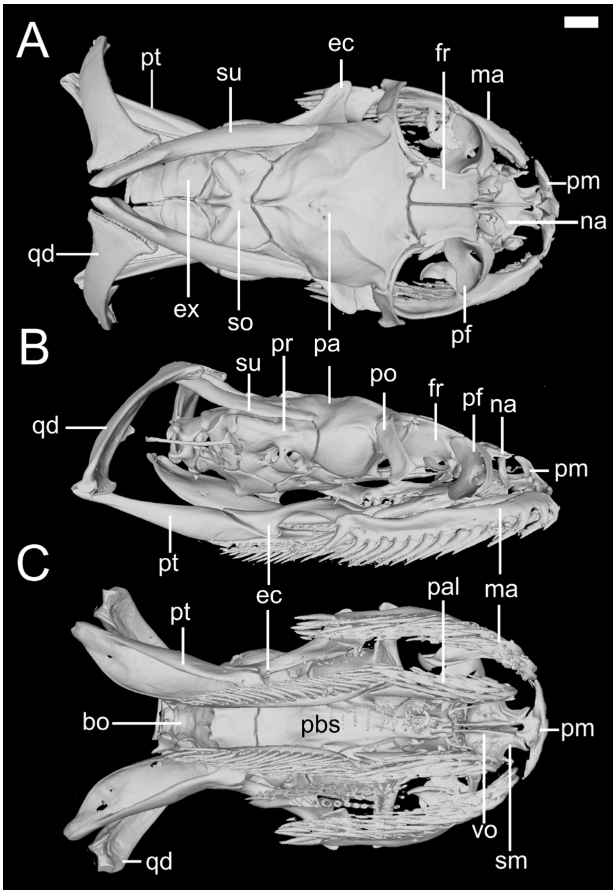

Figure 2. Three-dimensional reconstruction of the skull and suspensorium of *Helicops acangussu* (MPEG 25586) based on micro-computed tomography data. The mandible was digitally removed for better visualization. **A** – dorsal view; **B** – lateral view; **C** – ventral view. bo = basioccipital; ec = ectopterygoid; ex = exoccipital; fr = frontal; ma = maxilla; na = nasal; pa = parietal; pal = palatine; pbs = parabasisphenoid; pf = prefrontal; pm = premaxilla; po = postorbital; pr = prootic; pt = pterygoid; qd = quadrate; sm = septomaxilla; so = supraoccipital; su = supratemporal; vo = vomer. Scale = 1 mm.

]

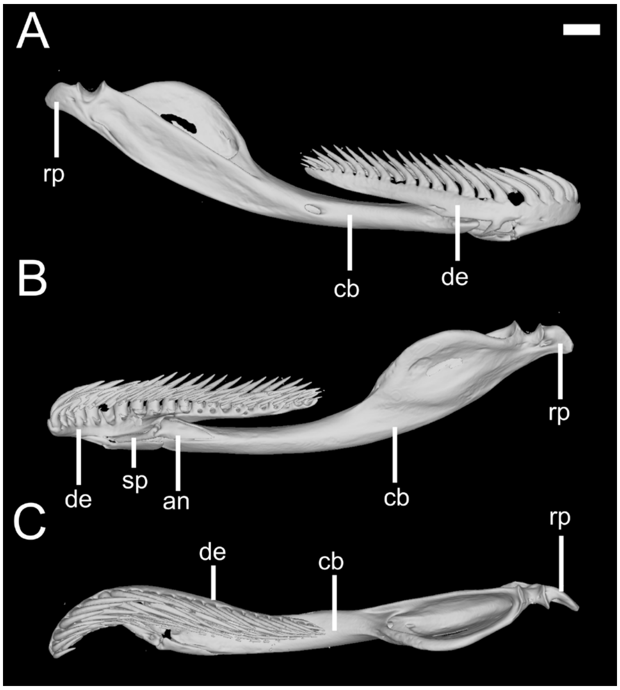

Figure 3. Three-dimensional reconstruction of the mandible of *Helicops acangussu* (MPEG 25586) based on micro-computed tomography data. Skull and suspensorium were digitally removed for better visualization. **A** – lateral view; **B** – medial view; **C** – dorsal view. an = angular; cb = compound bone; de = dentary; rp = retroarticular process; sp = splenial. Scale = 1 mm.

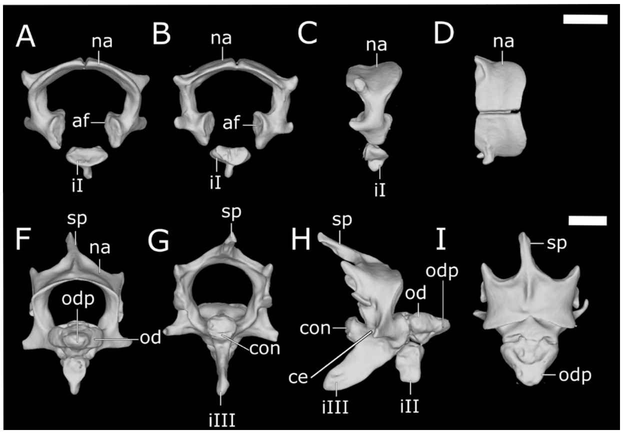

Figure 4. Three-dimensional reconstruction of the atlas and axis of *Helicops acangussu* (MPEG 25586) based on micro-computed tomography data. Skull, lower jaw and other vertebrae were digitally removed for better visualization. Atlas: **A** – anterior view; **B** – posterior view; **C** – lateral view; **D** – dorsal view. Axis: **F** – anterior view; **G** – posterior view; **H** – lateral view; **I** – dorsal view. af = articular facet; ce = centrum; con = occipital condyle; iI = intercentrum I; iII = intercentrum II; iIII = intercentrum III; na = neural arches; od = odontoid; odp = odontoid process; sp = spinal process. Scale = 1 mm.

first third of the hemipenial body in both organs. In specimen INPA 31415 (right), the total length of the hemipenes was 16 mm. Due to the imprecision of the lobe separation region, we did not measure this structure. The organ showed more variation than those from Leticia relative to the original species description (Figure 5). The lobes were not significantly asymmetrical, the distinction between the lobes and hemipenis body was unclear (capitation not detected). The central area of the asulcate face was covered mostly with spinules that invade the base of the lobes, and the base of the lobes on the asulcate face were surrounded by three small spinule rows followed by two rows of papillae (the last two near the apex) (Figure 5d). Irregular rows of small spinules were observed on the lobes and body of the hemipenis, except at the base, which was covered on its middle section by very small spicules and large spines arranged laterally (Figure 5d,e-f). The sulcate face had large spines arranged laterally at the basis, with evident spinules surrounding the spermatic sulcus and the intrasulcar region. The rows of spinules encircled both lobes, changing to rows of papillae at the apex (Figure 5d,e-f).

Material examined

(*skull and/or †hemipenis examined). BRAZIL: Amazonas: Tabatinga (SINCHI-R 1023); Presidente Figueiredo (INPA 31415*†); Rondônia: Porto Velho (MPEG 25586*); COLOMBIA: Amazonas: Leticia (SINCHI-R 1000, 1001, 1002, 1003, 1004, 1005, 1006, 1007, 1008, 1009, 1010, 1011, 1012, 1013, 1014, 1015, 1016, 1017, 1018, 1019, 1020, 1021, 1022, 1024, 1025†, 1026†, 1027, 1028, 1029, 2823, 3169, 3170).

Figure 5. Right hemipenes of *Helicops acangussu*. Specimen SINCHI-R 1025: **A** – sulcate; **B** – lateral view; **C** – assucalte faces. Specimen INPA 31415: **D** – sulcate; **E** – lateral view; **F** – asulcate face. Scale = 2 mm.

Distribution

We here expand the distribution of *H. acangussu* to the municipalities of Tabatinga and Presidente Figueiredo, in Amazonas State, Brazil, and to Letícia, in the Department of Amazonas, Colombia, the first country record of this species in Colombia. The new records imply an extension of the known distribution of the species by 818 km northwest and 907 km northeast from the type locality. All occurrences are in the Amazon Basin (Figure 6).

DISCUSSION

Moraes-da-Silva *et al.* (2022) suggested that *H. acangussu* is restricted to the left bank of the Madeira River and that large rivers may be essential factors to promote the vicariant speciation in *Helicops*. The new occurrence records reported in here refute large rivers as biogeographic barriers for *H. acangussu*, as both Leticia/Tabatinga and Presidente Figueiredo are located north of the Amazon River, while the Madeira River is a southern tributary to the Amazon, indicating that the species has a wide distribution within the Amazon Basin. Even though the formation of large-scale hydrographic basins may not have acted as barriers for this species, these basins may still serve as barriers for other watersnake species, such as *H. boitata* Moraes-da-Silva *et al.*, 2019 in the Paraguay Basin (Moraes-da-Silva *et al.* 2019) and *H. phantasma* Moraes-da-Silva *et al.*, 2021 in the Tocantins-Araguaia Basin (Moraes-da-Silva *et al.* 2021).

Some species of spotted-patterned *Helicops* that occur in remote areas are poorly represented in Brazilian scientific collections of large cities and museums (e.g., *H. yacu* and *H. petersi*) (Rossman and Dixon 1975; Rossman 1976; Rossman and Abe 1979). Therefore, the revision of material from regional collections (such as that of Instituto SINCHI in our case), which are more likely to house specimens from the surrounding environments, is essential to understand the distribution and taxonomy of these taxa (e.g., Trevine *et al.* 2021).

More data on skull morphology from other *Helicops* species and a molecular analysis will be necessary to clarify the kinship relationships of *H. acangussu*, since the spotted-patterned group is propably an artificial cluster (see Moraes-da-Silva *et al.* 2021). For instance, *H. acangussu* is sympatric not only with three spotted-patterned *Helicops* (*H. leopardinus*, *H. hagmanni*, and *H. polylepis*), as pointed out by Moraes-da-Silva *et al.* (2022). Our results indicate that it is also sympatric with *H. yacu* in the region of Leticia, Amazonas, Colombia (Rossman and Abe 1979). Among these species, only *H. acangussu* and *H. leopardinus* have moderate dorsal keels, unlike the others which have strong keels (Moraes-da-Silva *et al.* 2022). More extensive sampling efforts in the gap regions of their known distribution range is needed to assess more accurately the intraspecific morphological variation in these taxa.

Even though the knowledge on the skull anatomy of snakes has increased in the past decades, descriptive and detailed data on the osteology of *Helicops* are incipient, as most of the available data for the genus are related to contributions of wider systematic and/or evolutionary scope in snakes (e.g., Pietro *et al.* 2014; Klaczko *et al.* 2016). Thus, detailed descriptions for interspecific comparative purposes are still lacking. The data we present in here on the skull, lower jaw and cervical vertebrae shows that *H. acangussu* exhibitis a similar skull morphology in comparison to other congeners (i.e., *H. infrataeniatus* Jan, 1865, *H. leopardinus*

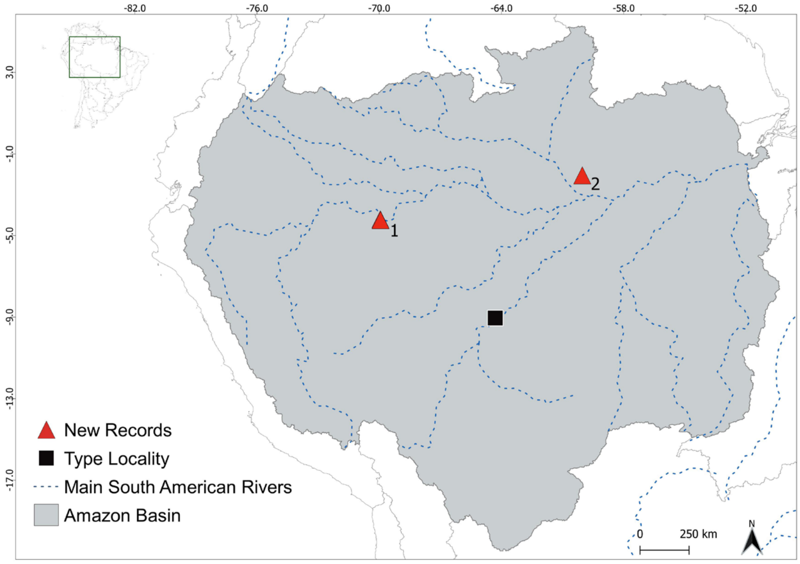

Figure 6. Map of the known distribution of *Helicops acangussu* showing its type locality and new locality records reported in here.

and *H. carinicaudus* Wied-Neuwied, 1824), also sharing some of the synapomorphies of the genus previously suggested in the literature, such as, as the pointed nasal, short vomerine processes, and a supratemporal of similar width along its length (Yuki and Lema 2005; Pietro *et al.* 2014). Additionally, *H. acangussu* presents small parietal foramina, a characteristic also consistently found in *H. leopardinus*, more variably in *H. infrataeniatus*, and also recorded in *H. carinicaudus* (Yuki and Lema 2005; Pietro *et al.* 2014).

Future systematic studies on the genus should include osteological data, as they are relevant for the systematics of cryptic species (e.g., Martins *et al.* 2019; 2023). Interspecific variation has already been detected in some characters of the skull such as the width of the anterior part of the external branch of the ectopterygoids, and other differences in the squamosal, palatine, and pterygoid bones between *H. carinicaudus* and *H. leopardinus* (Yuki and Lema 2005). Moreover, intraspecific variation should be considered, especially when osteological data are considered for broader systematic matters.

Postcranial osteology is rarely described in snakes in comparison to skull and mandible data, even though additional contributions have accumulated in the past decades with the aid of microCT scanning and 3D imaging (Bell *et al.* 2021; Szyndlar and Georgalis 2023). When considering post-cranial data, cervical (i.e., atlas and axis) vertebrae are the least studied amongst snakes, as they are known to be relatively morphologically conserved in comparison to precloacal vertebrae, and because they are seldom found in fossils (Holman 2000). The morphology of the atlas and axis in *H. acangussu* resembles the general pattern found in other dipsadids in that the atlas is a simplified vertebra lacking a neural spine and associated ribs, and that the axis bears a developed neural spine, an odontoid process oriented anteriorly and no associated ribs (Holman 2000; Szyndlar and Geogalis 2023). Even though our results indicate that the atlas and axis in *H. acangussu* have a similar pattern to that reported in the very few available studies on other species, recent studies with broader inter- and intraspecific samples (e.g., Martins *et al.* 2019; 2023) have shown that there is some degree of variation in the cervical vertebrae of other snake lineages, especially regarding the intercentra I, II and III, as well as the presence of rudimentary ribs associated to the axis that might be taxonomically informative. Additional studies focused on other squamate lineages (e.g., Araújo Salvino *et al.* 2024) revealed conspicuous morphological variation in the atlantoaxial region of amphisbaenids related to the head shape, indicating an intrinsic morphological association of these two osteological complexes. Thus, osteological studies on snakes should include post-cranial variation, as it might represent valuable data for the systematics and evolution within the group, especially considering the relevance for fossil lineages.

Finally, the examination of three additional hemipenes from other localities than the type locality showed a small level of intraspecific variation in hemipenial morphology for *H. acangussu* relative to the species description. We report the presence of symetrical hemipenial lobes, which contrasts with the asymmetry reported by Moraes-da-Silva *et al.* (2022). This contrast most likely represents an artifact in the hemipenis preparation for the species description, although further data are needed to endorse this affirmation, since we detected variation of hemipenial morphology in individuals of Presidente Figueiredo and Leticia and the lobes might be subject to intraspecific variation. Such a intraspecific variation in other internal morphological data of *Helicops* species were previously reported (Rossman 1976), but ecological and/or evolutive pressures underlying these variations remains poorly studied.

CONCLUSIONS

Our results indicate that *H. acangussu* is an Amazonian watersnake with a wide distribution in the Amazon Basin, occuring in sympatry with at least four other species of the spotted-paterened *Helicops* group. The species seems to present intraspecific geographical variation in hemipenial morphology. Our data showed that future studies on intraspecific variation in *Helicops* should focus on internal (e.g., skull and hemipenis) and external (e.g., pholidosis) morphology to more accurately contribute to the taxonomy and evolutionary relationships, as well as to the analysis of ecological patterns within the group.

ACKNOWLEDGMENTS

We are grateful to A. L. C. Prudente (MPEG) and F. Werneck (INPA) for access to specimens under their care. We are also grateful to Coordenação de Aperfeiçoamento de Pessoal de Nível Superior (CAPES) for financial support.

REFERENCES

Allsteadt, J.; Savitzky, A.H.; Petersen, C.E.; Naik, D.N. 2006. Geographic variation in the morphology of *Crotalus horridus* (Serpentes: Viperidae). *Herpetological Monographs* 20: 1–63. https://doi.org/10.1655/0733-1347(2007)20[1:GVITMO]2.0.CO;2

Araújo Salvino, C.; Hernandéz-Morales, C.; Daza, J.D.; Nunes, P.M.S. 2024. Comparative anatomy and evolution of the atlantoaxial complex in the fossorial lineage Amphisbaenia (Squamata: Lacertoidea). *The Anatomical Record* 307: 3623–3648.

Bell, C.; Daza, J.; Stanley, E.; Laver, R. 2021. Unveiling the elusive: X-rays bring scolecophidian snakes out of the dark. *The Anatomical Record* 304: 2110–2117.

Braz, H.B.; Scartozzoni, R.R.; Almeida-Santos, S.M. 2016. Reproductive modes of the South American water snakes: a study system for the evolution of viviparity in squamate reptiles. *Zoologischer Anzeiger* 263: 33–44.

Buser, T.J.; Boyd, O.F.; Cortés, Á.; Donatelli, C.M.; Kolmann, M.A.; Luparell, J.L.; Pfeiffenberger, J.A.; Sidlauskas, B.L.; Summers, A.P. 2020. The natural historian's guide to the CT galaxy: step-by-step instructions for preparing and analyzing computed tomographic (CT) data using cross-platform, open access software. *Integrative Organismal Biology* 2: obaa009.

Citeli, N.; Klaczko, J.; De-Lima, A.K.S.; de-Carvalho, M.; Nunes, P.M.S.; Passos, P.; Brandão, R.A. 2022. Taxonomy, allometry, sexual dimorphism, and conservation of the trans-Andean watersnake *Helicops danieli* Amaral, 1937 (Serpentes: Dipsadidae: Hydropsini). *Canadian Journal Zoology* 100: 184–196.

Costa, H.C.; Santana, D.J.; Leal, F.; Koroiva, R.; Garcia, P.C. 2016. A new species of *Helicops* (Serpentes: Dipsadidae: Hydropsini) from southeastern Brazil. Herpetologica 72: 157–166.

Cundall, D.; Irish, F. 2008. The snake skull. In: Gans, C.; Gaunt, A.S.; Adler, K. (Eds.). *Biology of the Reptilia*, v. 14. Society for the Study of Amphibians and Reptiles, New York, p.349-692.

Dowling, H.G. 1951. A proposed standard system of counting ventral in snakes. *British Journal of Herpetology* 1: 97–99.

Ennen, J.R.; Kalis, M.E.; Patterson, A.L.; Kreiser, B.R.; Lovich, J.E.; Godwin, J.; Qualls, C.P. 2014. Clinal variation or validation of a subspecies? A case study of the *Graptemys nigrinoda* complex (Testudines: Emydidae). *Biological Journal of the Linnean Society* 111: 810–822.

García-Cobos, D.; Crawford, A.J.; Ramírez-Pinilla, M.P. 2020. Reproductive phenology in a Neotropical aquatic snake shows marked seasonality influenced by rainfall patterns. *Journal of Natural History* 54: 1845–1862.

García-Cobos, D.; Gómez-Sánchez, D.A.; Crowe-Riddell, J.M.; Sanders, K.L.; Molina, J. 2022. Ecological and sexual roles of scale mechanoreceptors in two species of Neotropical freshwater snake (Dipsadinae: *Helicops*). *Biological Journal of the Linnean Society* 134: 958–974.

Holman, J.A. 2000. *Fossil Snakes of North America: Origin, Evolution, Distribution, Paleoecology.* Indiana University Press, Indiana, 317p.

Kawashita-Ribeiro, R. A.; Ávila, R.W.; Morais, D.H. 2013. A new snake of the genus *Helicops* Wagler, 1830 (Dipsadidae, Xenodontinae) from Brazil. *Herpetologica* 69: 80–90.

Klaczko, J.; Sherratt, E.; Setz, E.Z. 2016. Are diet preferences associated to skulls shape diversification in xenodontine snakes? PloS One 11: e0148375.

Lehner, B.; Grill, G. 2013. Global river hydrography and network routing: baseline data and new approaches to study the world's large river systems. *Hydrological Processes* 27: 2171–2186.

Martins, A.R.; Folly, M.; Ferreira, G.N.; Silva, A.S.G.; Koch, C.; Fouquet, A.; *et al.* 2023. An evolutionary paradox on threadsnakes: Phenotypic and molecular evidence reveal a new and remarkably polymorphic species of *Siagonodon* (Serpentes: Leptotyphlopidae: Epictinae) from Amazonia. *Vertebrate Zoology* 73: 345–366.

Martins, A.R.; Koch, C.; Pinto, R.; Folly, M.; Fouquet, A.; Passos, P. 2019. From the inside out: Discovery of a new genus of threadsnakes based on anatomical and molecular data, with discussion of the leptotyphlopid hemipenial morphology. *Journal of Zoological Systematics and Evolutionary Research* 57: 840–863.

Moraes-da-Silva, A.; Amaro, R.C.; Nunes, P.M.S.; Rodrigues, M.T.; Curcio, F.F. 2021. Long known, brand new, and possibly threatened: a new species of watersnake of the genus *Helicops* Wagler, 1828 (Serpentes; Xenodontinae) from the Tocantins-Araguaia River Basin, Brazil. *Zootaxa* 4903: 217–241.

Moraes-da-Silva, A.; Amaro, R.C.; Nunes, P.M.S.; Strüssmann, C.; Teixeira, M.J.; Andrade, A.J.; Curcio, F.F. 2019. Chance, luck and a fortunate finding: a new species of watersnake of the genus *Helicops* Wagler, 1828 (Serpentes: Xenodontinae), from the Brazilian Pantanal wetlands. *Zootaxa* 4651: 445–470.

Moraes-da-Silva, A.; Walterman, S.; Citeli, N.; Nunes, P.M.; Curcio, F.F. 2022. A new oviparous species of *Helicops* Wagler, 1828 (Serpentes, Xenodontinae) from Brazilian Amazonia with reflections on the evolution of viviparity among hydropsine watersnakes. *Zoologischer Anzeiger* 296: 91–109.

Nogueira, C.C.; Argôlo, A.S.J.; Arzamendia, V.; Azevedo, J.A.; Barbo, F.E.; Bérnils, R.S.; *et al.* 2019. Atlas of Brazilian snakes: Verified point-locality maps to mitigate the Wallacean shortfall in a megadiverse snake fauna. *South American Journal of Herpetology* 14(Special Issue 1): 1–274.

Pesantes O.S. 1994. A method for preparing the hemipenis of preserved snakes. *Journal of Herpetolology* 28: 93–95.

Pietro, D.O.D.; Alcalde, L.; Williams, J. 2014. New cranial characters in the tribe Hydropsini (Serpentes: Dipsadidae: Xenodontinae). *Acta Herpetologica* 9: 1–14.

Rasband, W.S. 2016. ImageJ. U.S. National Institutes of Health, Bethesda. (https://imagej.net/ij/). Accessed on 01 Mar 2020.

Rossman, D.A. 2002. Morphological variation in the endemic Colombian water snake, *Helicops danieli* Amaral, 1937 (Serpentes: Xenodontidae). *Revista de la Academia Colombiana de Ciencias Exactas, Físicas y Naturales* 26: 589–594.

Rossman, D.A. 1976. Revision of the South American colubrid snakes of the *Helicops pastazae* complex. *Occasional Papers of the Museum of Natural Science LSU* 50: 1–15.

Rossman, D.A.; Abe, A.S. 1979. Comments on the taxonomic status of *Helicops yacu* (Serpentes: Colubridae). *Proceedings of the National Academy of Sciences* 42: 7–9.

Rossman, D.A.; Dixon, J.R. 1975. A new colubrid snake of the genus *Helicops* from Peru. *Herpetologica* 31: 412–414.

Sabaj, M. 2020. Codes for natural history collections in ichthyology and herpetology. *Copeia* 108: 593–669.

Szyndlar, Z.; Georgalis, G.L. 2023. An illustrated atlas of the vertebral morphology of extant non-caenophidian snakes, with special emphasis on the cloacal and caudal portions of the column. *Vertebrate Zoology* 73: 717–886.

Trevine, V.C.; Caicedo-Portilla, J.R.; Hoogmoed, M.; Thomas, R.A.; Franco, F. L.; Montingelli, G.G.; Osorno-Muñoz, M.; Zaher, H. 2021. A new species of *Thamnodynastes* Wagler, 1830 from western Amazonia, with notes on morphology for members of the *Thamnodynastes pallidus* group (Serpentes, Dipsadidae, Tachymenini). *Zootaxa* 4952: 235–256.

Yuki, R.N.; Lema, T. 2005. Análise comparativa entre as cobras d'água meridionais (*Helicops carinicaudus* (Wied, 1825) e *H.*

infrataeniatus Jan, 1865) com a descrição do crânio e hemipênis (Serpentes: Colubridae: Xenodontinae). *Comunicações do Museu de Ciências e Tecnologia da PUCRS, Série Zoológica* 18: 85–128.

Zaher, H. 1999. Hemipenial morphology of the South American Xenodontine snakes, with a proposal for a monophyletic Xenodontinae and a reappraisal of colubroid hemipenis. Bulletin of the American Museum of Natural History 240: 1–168.

Zaher, H.; Prudente, A.L.C. 2003. Hemipenes of *Siphlophis* (Serpentes, Xenodontinae) and techniques of hemipenial preparation in snakes: a response to Dowling. *Herpetological Review* 34: 295–302

RECEIVED: 28/02/2024
ACCEPTED: 27/12/2024
ASSOCIATE EDITOR: Rafael de Fraga

DATA AVAILABILITY: The data that support the findings of this study are available upon request to the corresponding author [Nathalie Citeli].